Check for updates

Received: 12 January 2023 | Revised: 26 April 2023 | Accepted: 1 May 2023

DOI: 10.1111/ter.12664

RESEARCH ARTICLE

Terra Nova WILEY

Seismic evidence for ductile necking of the mid-lower crust beneath the Columbrets Basin (Western Mediterranean)

Adrià Ramos[1] | Antonio Pedrera[1] | Jesús García-Senz[1] | Berta López-Mir[1,2] | Ramon Salas[3]

[1]Instituto Geológico y Minero de España, Dpto. Geología y Subsuelo, CN IGME-CSIC, Madrid, Spain

[2]Dpto. Biología, Geología, Física y Química Inorgánica, Universidad Rey Juan Carlos, Madrid, Spain

[3]Departament de Mineralogia, Petrologia i Geologia Aplicada, Universitat de Barcelona, Barcelona, Spain

Correspondence
Adrià Ramos, Instituto Geológico y Minero de España, Dpto. Geología y Subsuelo, CN IGME-CSIC, Madrid, Spain.
Email: adria_ramos@outlook.com

Funding information
Spanish Science Ministry, Grant/Award Number: REViSE-Betics-PID2020-119651RBI00; Junta de Andalucía, Grant/Award Number: PY20-01387 and FIPS; IGME-CSIC, Grant/Award Number: Ayudas Extraordinarias Menciones Excelencia Severo Ochoa

Abstract

The Columbrets Basin is the largest Mesozoic rift basin of the Valencia Trough in the Western Mediterranean. The analysis of a seismic-reflection survey makes it possible to reconstruct the tectonic fabric underlying the sedimentary basin, including the structure of the top of the lower crust and the Moho. It is proposed that the ductile deformation of the mid-lower crust was the main mechanism controlling the basin geometry, with the radial flow of mid-lower crust coeval with the reactivation of two large-offset SW-dipping normal faults, inherited from the precursor Permian–Triassic rifting. Mid-lower crustal necking occurred below the major depocenters, immediately before hyperextension. Our results provide new insight into the formation of circular-shaped basins and the evolution of depth-dependent extensional processes during rifting.

KEYWORDS
Columbrets Basin, ductile deformation, extensional tectonics, mid-lower crustal thinning

1 | INTRODUCTION

Rift segmentation can be associated with pre-existing crustal heterogeneities. Likewise, extensional stresses concentrate along oblique inherited discontinuities, promoting en-echelon fault patterns (Jammes et al., 2009). The trend of those faults and their associated sedimentary depocentres lie between the strike of pre-existing crustal anisotropies and the vector orthogonal to the extension direction. In such scenarios, brittle faulting is often confined to the upper crust being coeval with plastic flow in the mid-lower crust (Brun et al., 2018; Clerc et al., 2018; Huismans & Beaumont, 2011). Thus, the upper crust could stretch and thin less than the entire crust, commonly referred to as a depth-dependent stretching mode (Davis & Kusznir, 2004; Huismans & Beaumont, 2011). One issue that may arise related to this process is the extensional discrepancy, which refers to the amount of crustal thinning not accounted for by the displacement of upper crustal faults. However, the structure and, consequently, the detailed behaviour of the mid-lower crust during rifting remain enigmatic, mainly due to the resolution and limited coverage of the available seismic surveys. Moreover, most examples describe successful hyperextended rifted margins such as the Gabon margin (Clerc et al., 2018) or the South China Sea (Zhao et al., 2021), where crustal extension culminated with mantle exhumation and oceanic spreading. Failed rift systems, alternatively, provide key observations to understand the structure and behaviour of the mid-lower crust structure prior to oceanization.

This is an open access article under the terms of the Creative Commons Attribution License, which permits use, distribution and reproduction in any medium, provided the original work is properly cited.
© 2023 The Authors. *Terra Nova* published by John Wiley & Sons Ltd.

The Mesozoic Columbrets Basin is an example of a Mesozoic oblique failed rift basin within the Western Mediterranean. A dense high-resolution 2D deep-seismic survey (SGV01 open file; Figure S1) makes it possible to visualize the structure of the sedimentary basin at the lithosphere scale, as well as the seismic signature of the Moho and the mid-lower crust. This paper presents a 3D reconstruction of the Columbrets Basin, together with sequential restoration of key seismic profiles, showing the lithosphere evolution from the Middle Jurassic to present-day. The main objectives are to discuss (i) the deformational mechanisms that led to crustal thinning, (ii) the behaviour of the mid-lower crust during oblique rifting and (iii) the localization of extension along inherited crustal-scale weak zones.

Statement of significance

The interpretation of a high-resolution 2D seismic-reflection survey across the Columbrets Basin allows reconstructing of the structure of the Moho and the top of the lower crust underneath and formulating a new kinematic model of evolution. Results identify a basin-bounding large-offset extensional fault that was coeval to the radial flow of the mid-lower crust. This mode of mid-lower crustal thinning provides new insight to understand the formation of circular-shaped basins and the evolution of depth-dependent extensional processes during rifting. Furthermore, our results have implications to constrain the linkage between the Tethys realm and the Iberian rift system in the kinematic reconstructions of eastern Iberia during the Mesozoic.

1.1 | The Columbrets Basin

The Columbrets Basin is located at the linking zone between the Iberian Chain, the Betic Cordillera and the Catalan Coastal Chain. It is surrounded

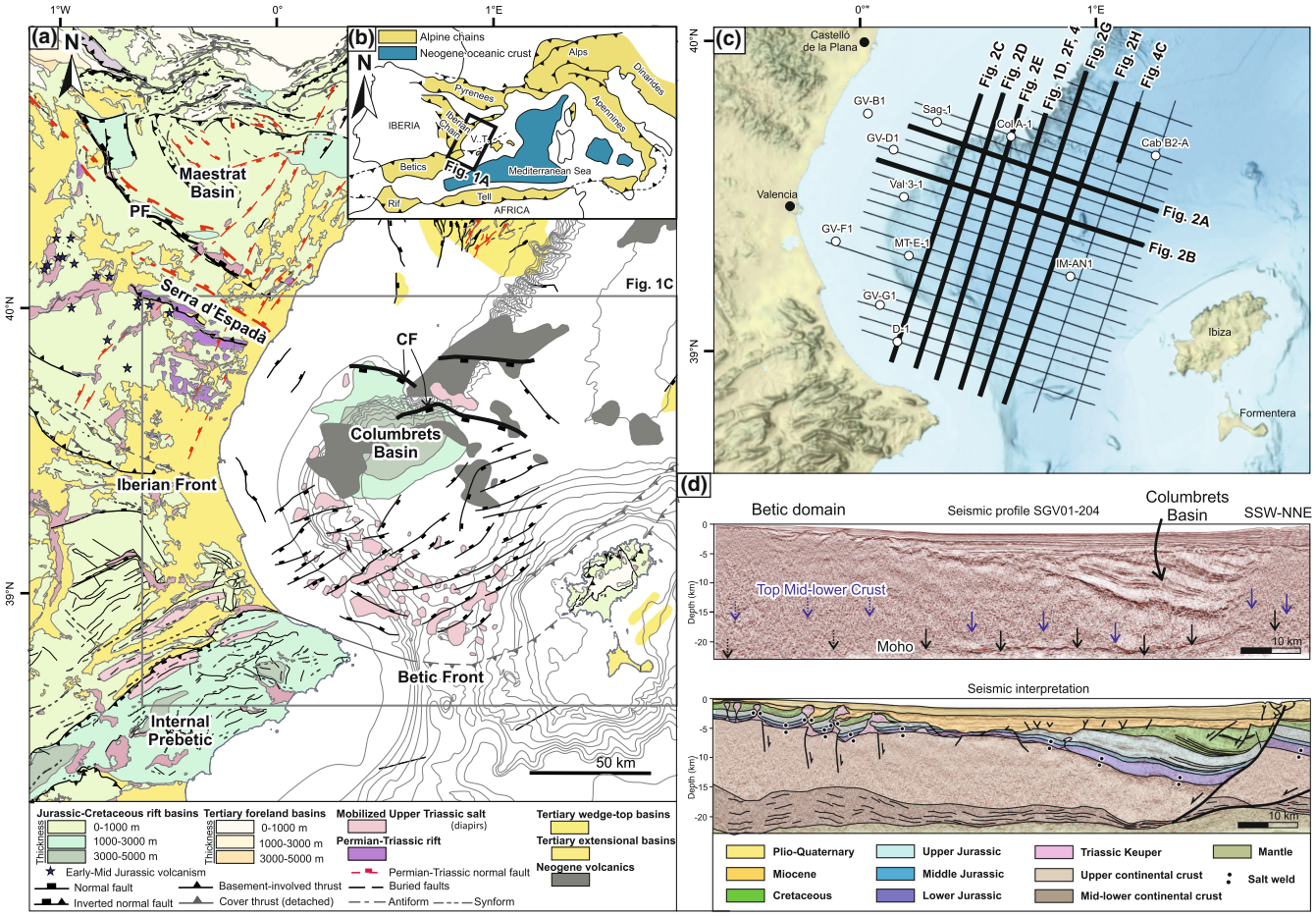

FIGURE 1 (a) Tectonic map of Eastern Iberia. (b) Simplified map of the Western Mediterranean and the Valencia Trough (VT) (modified from Roca et al., 1999). (c) Location of the seismic lines and well data used in this study. Well data (Lanaja, 1987): Cab B2-A: Cabriel B-1, Col A-1: Columbretes A-1, D-1: Denia-1, GV-B1: Golfo de Valencia B-1, GV-D1: Golfo de Valencia D-1, GV-F1: Golfo de Valencia F-1, GV-G1: Golfo de Valencia G-1, IM-AN1: Ibiza Marina AN-1, MT E-1: Marina del Turia E-1, Sag-1: Sagunto-1, V 3-1: Valencia 3-1. (d) 2D seismic profile used for sequential restorations in Figure 4. CF, Columbrets Fault; PF, Penyagolosa Fault. [Colour figure can be viewed at wileyonlinelibrary.com]

13653121, 2023, 5, Downloaded from https://onlinelibrary.wiley.com/doi/10.1111/ter.12664 by Universidad Rey Juan Carlos C/Tulipan S/N Edificio, Wiley Online Library on [28/11/2023]. See the Terms and Conditions (https://onlinelibrary.wiley.com/terms-and-conditions) on Wiley Online Library for rules of use; OA articles are governed by the applicable Creative Commons License

by the Maestrat and Internal Prebetic onshore basins. The sedimentary infill consists of a 15-km-thick Mesozoic to Cenozoic succession, deposited above a thinned continental crust (Etheve et al., 2018; Roma et al., 2018; Viñas-Gaza, 2016). The basin underwent two Mesozoic rifting events related to the opening of the Western Tethys and the Iberian intraplate rift, and a Cenozoic tectonic inversion event related to the convergence between Africa and Eurasia (Salas et al., 2001). Thus, the original basin was partially inverted during the formation of the Iberian Chain to the west (Guimerà, 2018) and the Betic Cordillera to the southwest (Etheve et al., 2016; Fontboté et al., 1990).

The precursor Late Permian to Early Triassic rifting phase, represented by the Buntsandstein facies (Vargas et al., 2009), is characterized by NW-SE and NE-SW high-angle faults, which are exposed throughout the Iberian Chain (Arche & López-Gómez, 1996) (Figure 1a). The following Middle-Late Triassic to Middle Jurassic post-rift phase is represented by Muschelkalk shales and limestones and Upper Triassic Keuper evaporitic unit of variable thickness, which is overlain by relative isopach Early and Middle Jurassic post-rift shallow-water carbonates (Salas et al., 2001). The Kimmeridgian to early Albian rifting event (Nebot & Guimerà, 2018; Salas et al., 2001; Salas et al., 2019) is represented by a 5–15-km-thick Upper Jurassic-Lower Cretaceous succession, consisting of platform carbonates that grade basinward to marlstones and are overlain by post-rift middle-late Albian and Upper Cretaceous carbonates. These Jurassic to Upper Cretaceous sedimentary successions are pierced by salt diapirs arising from the Upper Triassic salt layer (Vergés et al., 2020).

The basin experienced mild inversion during late Eocene-Aquitanian times marked by a regional-scale erosional unconformity. Tectonic inversion was followed by Early to Middle Miocene rapid subsidence, related to the onset of extension in the Valencia Trough, which is represented by 2–6 km of Lower Miocene platform carbonates and conglomerates, followed by Middle Miocene to recent clastic sediments (Ayala et al., 2015), separated by the Messinian unconformity (Roca et al., 1999). Such an extensional phase was accompanied by two Late Oligocene to Serravalian and Tortonian to present magmatic episodes (Martí et al., 1992) (Figures 1a and 2b).

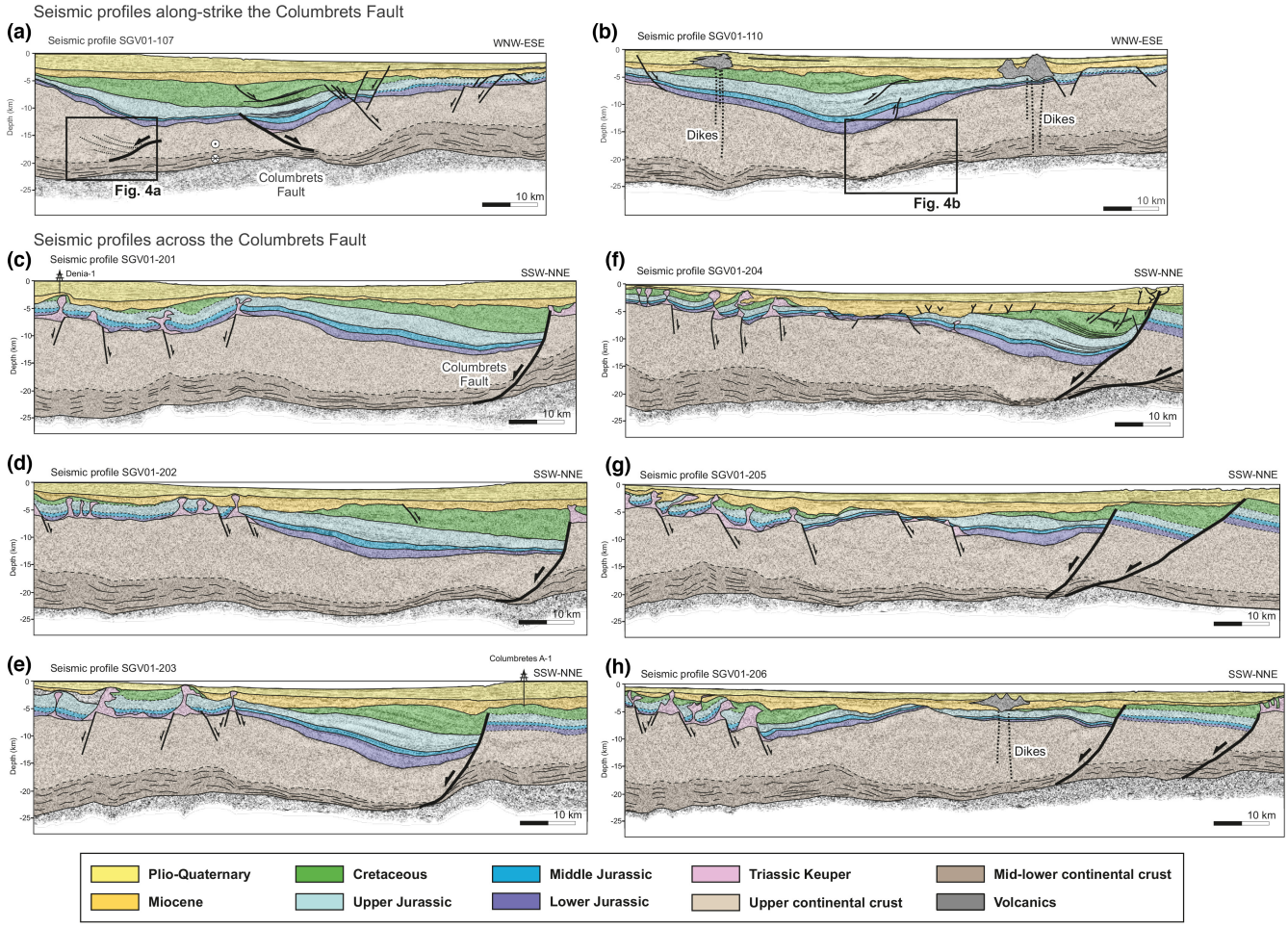

FIGURE 2 Depth-converted seismic interpretation of seismic profiles along-strike (a and b) and across (c-h) the Columbrets Fault. Notice that the fault throw decreases towards the east as the Mesozoic sedimentary package thins. Seismic profiles from the SGV01 survey were interpreted in time and converted to depth along with the interpreted horizons using interval velocities obtained from an available Expanded Spread Profile in the basin (ESP-7 in Torné et al., 1992; Pascal et al., 1992). Inferred Mesozoic horizons are mainly located in the southern part of the sections and are depicted by dashed black lines. See Figure 1c for the location. [Colour figure can be viewed at wileyonlinelibrary.com]

13653121, 2023, 5, Downloaded from https://onlinelibrary.wiley.com/doi/10.1111/ter.12664 by Universidad Rey Juan Carlos C/Tulipan S/N Edificio, Wiley Online Library on [28/11/2023]. See the Terms and Conditions (https://onlinelibrary.wiley.com/terms-and-conditions) on Wiley Online Library for rules of use; OA articles are governed by the applicable Creative Commons License

1.2 | Mesozoic crustal thinning in the Valencian Trough

Seismic lines show two WNW-ESE large-offset extensional faults separated by a relay zone affecting both the sedimentary cover and the entire crust in the northeastern basin margin (Figures 1a and 2). They show a domino-style faulting that produces tilting of upper crustal blocks. The cumulative large offset of faulting favours a sharp necking of the crust that thins from 19 km to less than 4 km (Figure 1d). The basin bounding fault (Columbrets Fault) includes two nearly parallel segments with an overlap zone and two Jurassic depocenters separated ~22 km (Figure 3b). Conversely, the thickest Cretaceous succession is found mostly on one depocenter located next to the bounding fault (Figure 3a). Secondary, NE-SW trending faults deform the hangingwall in the southern part of the Basin (Figure 3d). The distribution of Mesozoic depocenters and the thickness of the mid-lower crust are affected by this fault set.

The mid-lower crust shows planar fabric and narrow shear zones (Figure 4). In map view, it exhibits a circular shape (Figure 3e) and reaches less than 1 km underneath the syn-rift depocenters next to the Columbrets Fault (Figure 2f). The base of the lower crust is defined by a high-amplitude reflector, which remains largely flat and represents the Moho (e.g., Viñas-Gaza, 2016). Conversely, the top of the mid-lower crust is defined by an unfaulted moderate amplitude reflector that exhibits geometries indicative of ductile behaviour at ~15–17 km depth (Figure 3a). Above, the upper crust is rotated by 20° and displays sigmoidal reflectors, which are interpreted as drag folds associated with shearing above the mid-lower crust (Figure 4). Similar ductile thinning of the mid-lower crust has been documented in other seismic reflection and gravity modelling studies in the area (Dañobeitia et al., 1992; Torné et al., 1992).

1.3 | Tectonic evolution of the Columbrets Basin

The interpreted seismic profile SGV01-204 (Figure 1d) has been sequentially restored in six major steps (Figure 5) considering the depocenter thickness and distribution, and the timing of faulting, salt extrusion and welding: (i) Early-Middle Jurassic pre-rift, (ii) Late Jurassic stretching (onset of extension), (iii) Early Cretaceous thinning (main rifting event), (iv) Late Eocene–Oligocene folding and uplift (onset of shortening), (v) Miocene extension and (vi) Pliocene–Quaternary stage.

The Early-Middle Jurassic continental crustal thickness reaches up to 14–18 km (Figure 5f). The crust thins eastwards, towards the area occupied by the major normal faults in subsequent evolutionary stages. The Triassic salt and the Lower-Middle Jurassic succession fill sag depressions where the salt unit reaches up to 2500 m. Overall, these trends suggest that, prior to the onset of extension, the deposition of Lower-Middle Jurassic strata was already controlled by salt expulsion towards the basin's borders, such as the northern one where the Jurassic succession is not preserved.

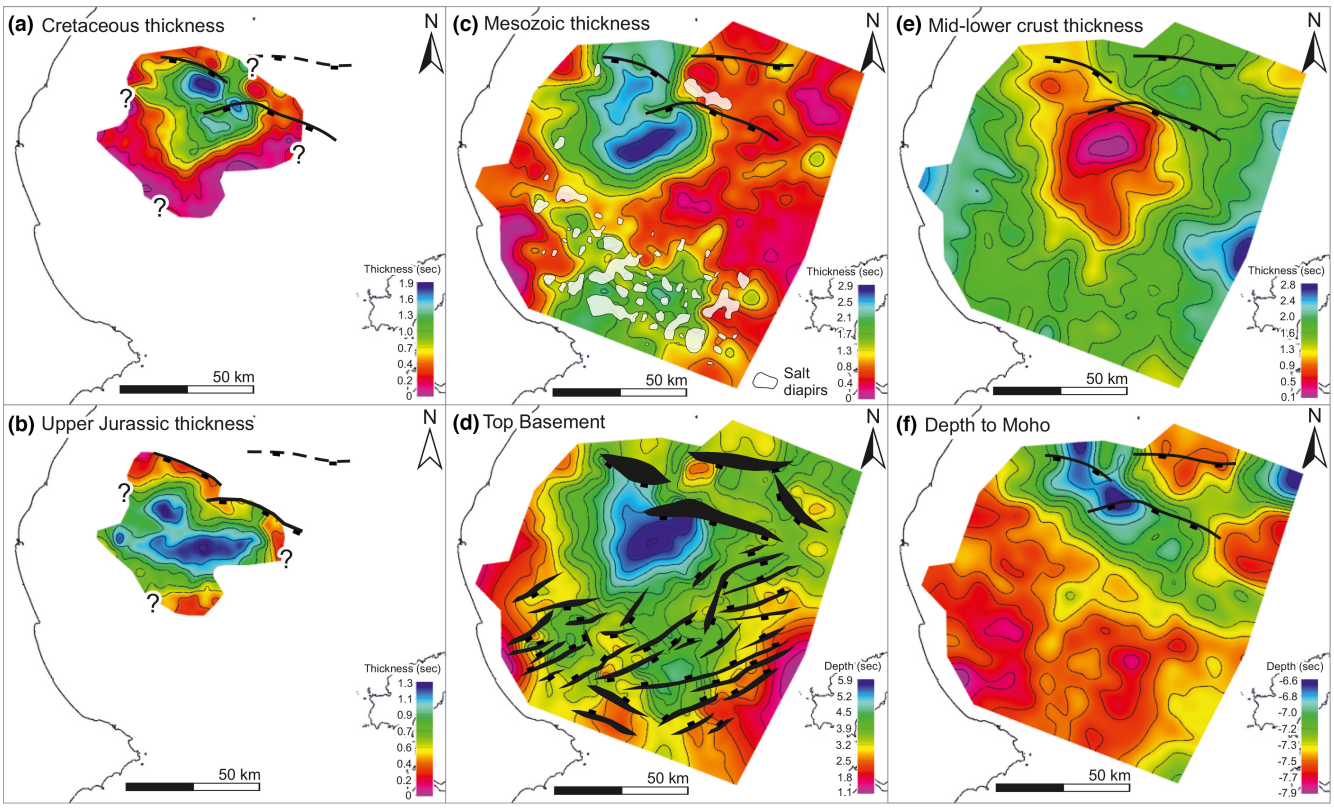

FIGURE 3 Structural TWT maps of Cretaceous (a), Upper Jurassic (b), Mesozoic (c) and mid-lower crust (e) thickness; and depth structural maps of the top of the basement (d) and the top of the Moho (f). [Colour figure can be viewed at wileyonlinelibrary.com]

13653121, 2023, 5, Downloaded from https://onlinelibrary.wiley.com/doi/10.1111/ter.12664 by Universidad Rey Juan Carlos C/Tulipan S/N Edificio, Wiley Online Library on [28/11/2023]. See the Terms and Conditions (https://onlinelibrary.wiley.com/terms-and-conditions) on Wiley Online Library for rules of use; OA articles are governed by the applicable Creative Commons License

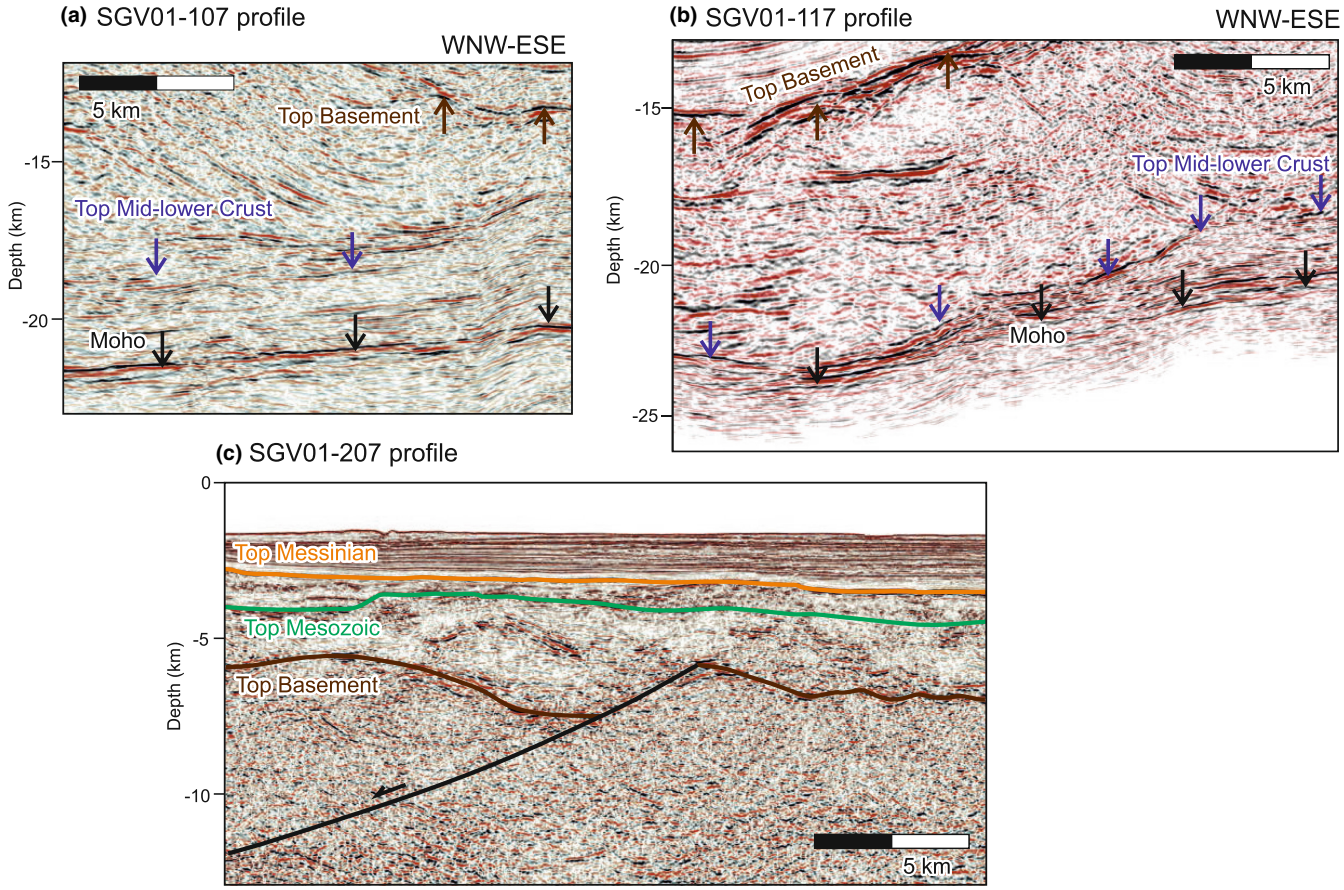

FIGURE 4 Zoom to the 2D seismic profiles of Figure 2b, showing the extensional geometries in the lower part of the crust (a and b). (c) Detail of a basement-involved oblique fault. [Colour figure can be viewed at wileyonlinelibrary.com]

The main tectonic extension, reflecting the coupling between the sedimentary cover and the basement (Motus et al., 2022), is attested by thickness variations of the Late Jurassic succession, ranging from 100 to 4200 m (Figure 5e). Onlap geometries and rollover synclines are indicative of moderate salt expulsion northward, which contributed to the creation of accommodation space and culminated with the progressive touchdown of the basin on the basement. In addition, high-angle oblique basement faults nucleate diapiric structures to the south, at the eastern prolongation of the Prebetic domain.

The maximum amount of thinning of the mid-lower crust is observed in the Early Cretaceous reconstruction (Figure 5d), with crustal thickness decreasing from 11 km in the previous Late Jurassic stage to only 7 km. Crustal thinning was mainly accommodated by two SW-dipping listric faults separated by a relay ramp (Figure 5d). Fault activity migrates to the north during progressive extension (Figure 5d,e).

Following rifting, the southern basin margin underwent domal uplift, as recorded by a regional unconformity eroding up to 3700 m of Jurassic and Cretaceous strata (Figure 5c,d). Such uplift is related to the tectonic inversion of the Maestrat and Cameros basins in the Iberian Cordillera from the Late Eocene to the Aquitanian (Early Miocene) (Nebot & Guimerà, 2016; Rat et al., 2019). The maximum erosion took place in the transition zone between the Columbrets Basin (Iberian domain) and the Betic domain, now overlain by Miocene strata from the continental margin (Figure 5c).

Continental margin flexure at the Miocene accommodated by shallow-dipping extensional faults occurred synchronously to the inversion stage of the Prebetic domain (Pedrera et al., 2014), which squeezed the diapirs at the southern segment of the restored cross-section (Figure 5b). It is worth noting that the Neogene sedimentary succession reaches a maximum thickness of 3500 m in the transition zone between the Columbrets Basin and the Betic domain, matching the maximum erosion of the preceding uplift stage (Figure 5b,c).

The present-day structure exhibits minor normal faults associated with a Pliocene-Quaternary diffuse extensional event, during which the main basin-bounding faults experience minor reactivations (Figure 5a).

2 | DISCUSSION AND CONCLUSIONS

The published models that deal with the structure and evolution of the Columbrets Basin can be grouped into three main categories. The first one considers a large NW-dipping extensional detachment

13653121, 2023, 5, Downloaded from https://onlinelibrary.wiley.com/doi/10.1111/ter.12664 by Universidad Rey Juan Carlos C/Tulipan S/N Edificio, Wiley Online Library on [28/11/2023]. See the Terms and Conditions (https://onlinelibrary.wiley.com/terms-and-conditions) on Wiley Online Library for rules of use; OA articles are governed by the applicable Creative Commons License

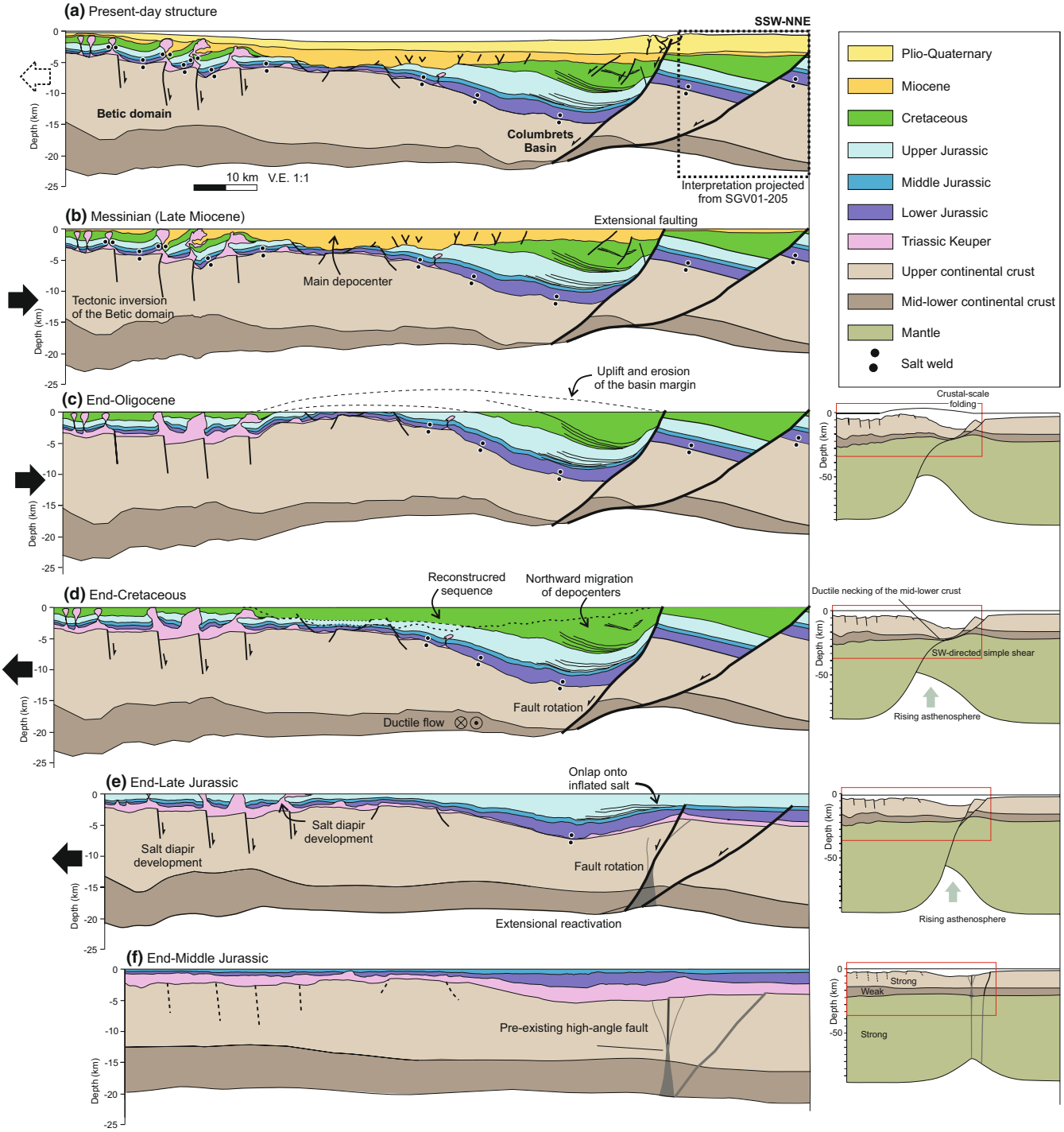

FIGURE 5 Sequential structural restoration of the depth-converted interpreted seismic profiles SGV01-204 and SGV01-205 (projected ~9 km in the northern part of the cross-section). Six evolutionary stages are depicted: (a) present-day, (b) Miocene, (c) Oligocene, (d) Early Cretaceous, (e) Late Jurassic, (f) Early-Middle Jurassic, together with the evolution of the lithosphere (right-hand side). The evolution of the lithosphere is sketched on the right-hand side. See Figure 1c for location. The restoration workflow follows the methodology by Ramos et al. (2020), taking into account the sedimentary decompaction of each stratigraphic interval and compaction curves for average lithologies. Percentage lithologies and average density values were calculated using nearby well data (Lanaja, 1987). Vertical scale is placed in the restoration steps for depth reference and does not represent the paleobathymetry in each time step. [Colour figure can be viewed at wileyonlinelibrary.com]

underlying the SE border of the basin (Etheve et al., 2018; Fang et al., 2021). The second considers an SE-dipping low-angle ramp/flat extensional intracrustal fault, which accommodated 80 km of displacement, along with salt migration and decoupling (Roma et al., 2018). The third suggests the coupling between the upper crust and the mantle along an SE-dipping shear zone (Granado

13653121, 2023, 5, Downloaded from https://onlinelibrary.wiley.com/doi/10.1111/ter.12664 by Universidad Rey Juan Carlos C/Tulipan S/N Edificio, Wiley Online Library on [28/11/2023]. See the Terms and Conditions (https://onlinelibrary.wiley.com/terms-and-conditions) on Wiley Online Library for rules of use; OA articles are governed by the applicable Creative Commons License

et al., 2016). In this work, the strain is localized along two SW-dipping basin-boundary faults. They show a domino style with stair-step pattern of tilted crustal blocks accompanied by ductile flow within the mid-lower crust. The combination of both processes led to subsidence and the formation of the circular pattern of the Columbrets Basin.

Furthermore, the occurrence of parallel Permo-Triassic structures onshore and Early-Mid Jurassic volcanism in the Serra d'Espadà, in the Central Iberian rift system (Salas et al., 2001; Figure 1a), suggests that the WNW-ESE trend of these large-offset faults is likely inherited from pre-existing basement-involved faults. These pre-existing faults represent the northern boundary of the ENE-WSW oblique fault system, which nucleated diapiric structures to the south but did not generate major thickness changes within the Columbrets Basin or the mid-lower crust (Figure 3c).

Brittle deformation in the upper crust appears to be accompanied by the ductile necking of the mid-lower crust (Figure 5). This mode of deformation is probably related to the ductile rheological behaviour of a felsic composition of the mid-lower crust during extension (Weinberg et al., 2007). Necking near the base of the crust was probably favoured by high temperatures produced by the rising asthenosphere (Huismans & Beaumont, 2011), which would significantly reduce the viscosity and favour ductile flow deformation beneath ~17 km (Figure 5). The fact that the shallowest Moho extends along a WNW-ESE band, matching the trace of the master fault (Figure 3f), together with the circular thinning pattern of the top of the mid-lower crust (Figure 3e), suggests that oblate extension and radial flow prevailed at lower crustal levels, while SSW-directed extension prevailed in the upper crust and the mantle lithosphere. Ductile flow within the mid-lower crust may have been the primary control on the formation of the circular-shaped basin. Further geophysical data could help to refine the geodynamical mechanisms behind the formation of these types of basins.

In summary, it is suggested that strain localization along a pre-existing high-angle fault evolved from a reactivated steeply-dipping fault to a crustal-scale shear zone. The increased viscosity related to a high thermal gradient promoted ductile flow within the mid-lower crust, leading to crustal necking immediately before hyperextension. Our results provide an exceptional example of depth-dependent stretching, where 80% of thinning is accommodated by ductile deformation in the mid-lower crust and the remaining 20% by extensional faulting in the upper crust. This mode of mid-lower crustal thinning may provide new insight to understand the formation of circular-shaped basins and the evolution of depth-dependent extensional processes during rifting.

On the other hand, most of the published kinematic reconstructions of the West Mediterranean region show a gap in this sector of the Tethys realm, so the linkage between the Tethys and the Iberian rift system remains largely unconstrained (Angrand et al., 2020; Angrand & Mouthereau, 2021; Nirrengarten et al., 2018; Pedrera et al., 2020; Tavani et al., 2018). The findings of this work can help to pinpoint the kinematic plate reconstructions in eastern Iberia during the Mesozoic. Some of these reconstructions emphasize the role of the Permian–Triassic diffuse rift system in the nucleation and development of extensional basins during the Mesozoic (e.g., Angrand & Mouthereau, 2021), which are in line with our results.

ACKNOWLEDGEMENTS

This work is part of the projects REViSE-Betics-PID2020-119651RBI00 (Spanish Science Ministry) and FIPS, PY20-01387 (Junta de Andalucía), also funded by the 'Ayudas Extraordinarias Menciones Excelencia Severo Ochoa' (IGME-CSIC). We thank Stefano Tavani, F. Mouthereau and an anonymous reviewer for their constructive comments and suggestions on the manuscript.

DATA AVAILABILITY STATEMENT

The data that support the findings of this study are openly available in Base de Datoby the Spanish Ministry of Ecological Transition at https://datos.gob.es/es/catalogo/ea0010987-base-de-datos-de-hidrocarburos.

REFERENCES

Angrand, P., & Mouthereau, F. (2021). Evolution of the Alpine orogenic belts in the Western Mediterranean region as resolved by the kinematics of the Europe-Africa diffuse plate boundary. *Bulletin de la Société Géologique de France*, *192*, 42. https://doi.org/10.1051/bsgf/2021031

Angrand, P., Mouthereau, F., Masini, E., & Asti, R. (2020). A reconstruction of Iberia accounting for Western Tethys–North Atlantic kinematics since the late-Permian–Triassic. *Solid Earth*, *11*, 1313–1332. https://doi.org/10.5194/se-11-1313-2020

Arche, A., & López-Gómez, J. (1996). Origin of the Permian-Triassic Iberian Basin, Central-Eastern Spain. *Tectonophysics*, *266*, 443–464. https://doi.org/10.1016/S0040-1951(96)00202-8

Ayala, C., Torne, M., & Roca, E. (2015). A review of the current knowledge of the crustal and lithospheric structure of the Valencia Trough Basin. *Boletín geológico y Minero*, *126*, 533–552.

Brun, J.-P., Sokoutis, D., Tirel, C., Gueydan, F., Van Den Driessche, J., & Beslier, M.-O. (2018). Crustal versus mantle core complexes. *Tectonophysics*, *746*, 22–45. https://doi.org/10.1016/j.tecto.2017.09.017

Clerc, C., Ringenbach, J.-C., Jolivet, L., & Ballard, J.-F. (2018). Rifted margins: Ductile deformation, boudinage, continentward-dipping normal faults and the role of the weak lower crust. *Gondwana Research*, *53*, 20–40. https://doi.org/10.1016/j.gr.2017.04.030

Dañobeitia, J. J., Arguedas, M., Gallart, J., Banda, E., & Makris, J. (1992). Deep crustal configuration of the Valencia trough and its Iberian and Balearic borders from extensive refraction and wide-angle reflection seismic profiling. *Tectonophysics*, *203*, 37–55. https://doi.org/10.1016/0040-1951(92)90214-Q

Davis, M., & Kusznir, N. (2004). Depth-dependent lithospheric stretching at rifted continental margins. In G. D. Karner, B. Taylor, N. W. Driscoll, & D. L. Kohlstedt (Eds.), *Rheology and deformation of the lithosphere at continental margins*. Columbia University Press, New York Chichester.

Etheve, N., Frizon de Lamotte, D., Mohn, G., Martos, R., Roca, E., & Blanpied, C. (2016). Extensional vs contractional Cenozoic deformation in Ibiza (Balearic promontory, Spain): Integration in the West Mediterranean back-arc setting. *Tectonophysics*, *682*, 35–55. https://doi.org/10.1016/j.tecto.2016.05.037

13653121, 2023, 5, Downloaded from https://onlinelibrary.wiley.com/doi/10.1111/ter.12664 by Universidad Rey Juan Carlos C/Tulipan S/N Edificio, Wiley Online Library on [28/11/2023]. See the Terms and Conditions (https://onlinelibrary.wiley.com/terms-and-conditions) on Wiley Online Library for rules of use; OA articles are governed by the applicable Creative Commons License

Etheve, N., Mohn, G., Frizon de Lamotte, D., Roca, E., Tugend, J., & Gómez-Romeu, J. (2018). Extreme Mesozoic crustal thinning in the eastern Iberia margin: The example of the Columbrets Basin (Valencia trough). *Tectonics*, *37*, 636–662. https://doi.org/10.1002/2017TC004613

Fang, P., Tugend, J., Mohn, G., Kusznir, N., & Ding, W. (2021). Evidence for rapid large-amplitude vertical motions in the Valencia trough (Western Mediterranean) generated by 3D subduction slab rollback. *Earth and Planetary Science Letters*, *575*, 117179. https://doi.org/10.1016/j.epsl.2021.117179

Fontboté, J. M., Guimerà, J., Roca, E., Sàbat, F., Santanach, P., & Fernandez-Ortigosa, F. (1990). The Cenozoic geodynamic evolution of the Valencia trough (Western Mediterranean). *Revista de la Sociedad Geológica de España*, *3*, 249–259.

Granado, P., Urgeles, R., Sàbat, F., Albert-Villanueva, E., Roca, E., Muñoz, J. A., Mazzuca, N., & Gambini, R. (2016). Geodynamical framework and hydrocarbon plays of a salt giant: The NW Mediterranean Basin. *Petroleum Geoscience*, *22*, 309–321. https://doi.org/10.1144/petgeo2015-084

Guimerà, J. J. (2018). Structure of an intraplate fold-and-thrust belt: The Iberian chain. A Synthesis. *Geologica Acta*, *16*, 427–438. https://doi.org/10.1344/GeologicaActa2018.16.4.6

Huismans, R., & Beaumont, C. (2011). Depth-dependent extension, two-stage breakup and cratonic underplating at rifted margins. *Nature*, *473*, 74–78. https://doi.org/10.1038/nature09988

Jammes, S., Manatschal, G., Lavier, L., & Masini, E. (2009). Tectonosedimentary evolution related to extreme crustal thinning ahead of a propagating ocean: Example of the western Pyrenees. *Tectonics*, *28*, TC4012. https://doi.org/10.1029/2008TC002406

Lanaja, J. M. (1987). *Contribución de la exploracíon petrolífera al conocimiento de la geología de España*. Instituto Geologico y Minero de España (IGME).

Martí, J., Mitjavila, J., Roca, E., & Aparicio, A. (1992). Cenozoic magmatism of the Valencia trough (Western Mediterranean): Relationship between structural evolution and volcanism*. *Tectonophysics*, *203*, 145–165. https://doi.org/10.1016/0040-1951(92)90221-Q

Motus, M., Nardin, E., Mouthereau, F., & Denèle, Y. (2022). Evolution of rift-related cover-basement decoupling revealed by brecciation processes in the eastern Pyrenees. *BSGF - Earth Sciences Bulletin*, *193*, 14. https://doi.org/10.1051/bsgf/2022013

Nebot, M., & Guimerà, J. (2016). Structure of an inverted basin from subsurface and field data: The late Jurassic-early cretaceous Maestrat Basin (Iberian chain). *Geologica Acta*, *14*, 155–177. https://doi.org/10.1344/GeologicaActa2016.14.2.5

Nebot, M., & Guimerà, J. (2018). Kinematic evolution of a fold-and-thrust belt developed during basin inversion: The Mesozoic Maestrat basin, E Iberian Chain. *Geological Magazine*, *155*, 630–640. https://doi.org/10.1017/S001675681600090X

Nirrengarten, M., Manatschal, G., Tugend, J., Kusznir, N., & Sauter, D. (2018). Kinematic evolution of the southern North Atlantic: Implications for the formation of hyperextended rift systems. *Tectonics*, *37*, 89–118. https://doi.org/10.1002/2017TC004495

Pascal, G., Torné, M., Buhl, P., Watts, A. B., & Mauffret, A. (1992). Crustal and velocity structure of the Valencia trough (western Mediterranean), part II. Detailed interpretation of five expanded spread profiles. *Tectonophysics*, *203*, 21–35. https://doi.org/10.1016/0040-1951(92)90213-P

Pedrera, A., Marín-Lechado, C., Galindo-Zaldívar, J., & García-Lobón, J. L. (2014). Control of preexisting faults and near-surface diapirs on geometry and kinematics of fold-and-thrust belts (internal Prebetic, eastern Betic cordillera). *Journal of Geodynamics*, *77*, 135–148. https://doi.org/10.1016/j.jog.2013.09.007

Pedrera, A., Ruiz-Constán, A., García-Senz, J., Azor, A., Marín-Lechado, C., Ayala, C., Díaz de Neira, J. A., & Rodríguez-Fernández, L. R. (2020). Evolution of the south-Iberian paleomargin: From hyperextension to continental subduction. *Journal of Structural Geology*, *138*, 104122. https://doi.org/10.1016/j.jsg.2020.104122

Ramos, A., Fernández, O., Terrinha, P., Muñoz, J. A., & Arnaiz, Á. (2020). Paleogeographic evolution of a segmented oblique passive margin: The case of the SW Iberian margin. *International Journal of Earth Sciences*, *109*, 1871–1895. https://doi.org/10.1007/s00531-020-01878-w

Rat, J., Mouthereau, F., Brichau, S., Crémades, A., Bernet, M., Balvay, M., Ganne, J., Lahfid, A., & Gautheron, C. (2019). Tectonothermal evolution of the Cameros Basin: Implications for tectonics of North Iberia. *Tectonics*, *38*, 440–469. https://doi.org/10.1029/2018TC005294

Roca, E., Sans, M., Cabrera, L., & Marzo, M. (1999). Oligocene to middle Miocene evolution of the central Catalan margin (Northwestern Mediterranean). *Tectonophysics*, *315*, 209–229. https://doi.org/10.1016/S0040-1951(99)00289-9

Roma, M., Ferrer, O., Roca, E., Pla, O., Escosa, F. O., & Butillé, M. (2018). Formation and inversion of salt-detached ramp-syncline basins. Results from analog modeling and application to the Columbrets Basin (Western Mediterranean). *Tectonophysics*, *745*, 214–228. https://doi.org/10.1016/j.tecto.2018.08.012

Salas, R., Guimerà, J., Bover-Arnal, T. Y, & Nebot, M. (2019). The Iberian-Catalan linkage: The Maestrat and Garraf basins. In: C. Quesada & J. T. Oliveira (Eds.), *The geology of Iberia: A geodynamic approach*, *regional geology reviews*, *volume 3: The Alpine Cycle*, *The Late Jurassic–Early Cretaceous Rifting* (pp. 228–231). Springer.

Salas, R., Guimerà, J., Mas, R., Martin-Closas, C., Meléndez, A., & Alonso, A. (2001). Evolution of the Mesozoic central Iberian rift system and its Cainozoic inversion (Iberian chain). In P. A. Ziegler, W. Cavazza, A. H. F. Robertson, & S. Crasquin-Soleau (Eds.), *Peri-Tethys Memoir*, *6: Peri-Tethyan Rift/Wrench Basins and Passive Margins*. *Mémoires du Muséum national d'Histoire naturelle* (pp. 145–186). 186 Publ. scientifiques du Muséum.

Tavani, S., Bertok, C., Granado, P., Piana, F., Salas, R., Vigna, B., & Muñoz, J. A. (2018). The Iberia-Eurasia plate boundary east of the Pyrenees. *Earth-Science Reviews*, *187*, 314–337. https://doi.org/10.1016/j.earscirev.2018.10.008

Torné, M., Pascal, G., Buhl, P., Watts, A. B., & Mauffret, A. (1992). Crustal and velocity structure of the Valencia trough (western Mediterranean), part I. A Combined Refraction/ Wide-Angle Reflection and near-Vertical Reflection Study. *Tectonophysics*, *203*, 1–20. https://doi.org/10.1016/0040-1951(92)90212-O

Vargas, H., Gaspar-Escribano, J. M., López-Gómez, J., Van Wees, J.-D., Cloetingh, S., de La Horra, R., & Arche, A. (2009). A comparison of the Iberian and Ebro basins during the Permian and Triassic, eastern Spain: A quantitative subsidence modelling approach. *Tectonophysics*, *474*, 160–183. https://doi.org/10.1016/j.tecto.2008.06.005

Vergés, J., Poprawski, Y., Almar, Y., Drzewiecki, P. A., Moragas, M., Bover-Arnal, T., Macchiavelli, C., Wright, W., Messager, G., Embry, J., & Hunt, D. (2020). Tectono-sedimentary evolution of Jurassic–Cretaceous diapiric structures: Miravete anticline, Maestrat Basin, Spain. *Basin Research*, *32*, 1653–1684. https://doi.org/10.1111/bre.12447

Viñas-Gaza, M. (2016). *Tectonic structure and formation kinematics of the Western Mediterranean basins*. PhD Thesis, Universitat de Barcelona, 226.

Weinberg, R. F., Regenauer-Lieb, K., & Rosenbaum, G. (2007). Mantle detachment faults and the breakup of cold continental lithosphere. *Geology*, *35*, 1035. https://doi.org/10.1130/G23918A.1

13653121, 2023, 5, Downloaded from https://onlinelibrary.wiley.com/doi/10.1111/ter.12664 by Universidad Rey Juan Carlos C/Tulipan S/N Edificio, Wiley Online Library on [28/11/2023]. See the Terms and Conditions (https://onlinelibrary.wiley.com/terms-and-conditions) on Wiley Online Library for rules of use; OA articles are governed by the applicable Creative Commons License

Zhao, Y., Ding, W., Ren, J., Li, J., Tong, D., & Zhang, J. (2021). Extension discrepancy of the hyper-thinned continental crust in the Baiyun rift, northern margin of the South China Sea. *Tectonics*, *40*, e2020TC006547. https://doi.org/10.1029/2020TC006547

SUPPORTING INFORMATION

Additional supporting information can be found online in the Supporting Information section at the end of this article.

How to cite this article: Ramos, A., Pedrera, A., García-Senz, J., López-Mir, B., & Salas, R. (2023). Seismic evidence for ductile necking of the mid-lower crust beneath the Columbrets Basin (Western Mediterranean). *Terra Nova*, *35*, 404–412. https://doi.org/10.1111/ter.12664

13653121, 2023, 5, Downloaded from https://onlinelibrary.wiley.com/doi/10.1111/ter.12664 by Universidad Rey Juan Carlos C/Tulipan S/N Edificio, Wiley Online Library on [28/11/2023]. See the Terms and Conditions (https://onlinelibrary.wiley.com/terms-and-conditions) on Wiley Online Library for rules of use; OA articles are governed by the applicable Creative Commons License